Available online at www.sciencedirect.com

ScienceDirect

Ceramics International 36 (2010) 1091–1094

CERAMICS
INTERNATIONAL

www.elsevier.com/locate/ceramint

# Structure and luminescence of $Eu^{3+}$ doped glass ceramics embedding ZnO quantum dots

Yunlong Yu, Daqin Chen, Ping Huang, Hang Lin, Yuansheng Wang *

*State Key Laboratory of Structural Chemistry, Fujian Institute of Research on the Structure of Matter, Chinese Academy of Sciences, Fuzhou, China*

Received 23 September 2009; received in revised form 12 October 2009; accepted 24 November 2009

**Abstract**

$Eu^{3+}$ doped glass ceramics embedding ZnO quantum dots (QDs) were successfully prepared by a sol–gel method. High-resolution transmission electron microscopy (HRTEM) observations revealed that ZnO QDs with size of 3–6 nm precipitated homogeneously among the $SiO_2$ glassy matrix after thermal treatment of the precursor sample. Such glass ceramics show a high transparency in the visible-infrared range due to the much smaller size of the ZnO QDs than the wavelength of the visible light. The emission and excitation spectra of the samples with various ZnO contents were studied. Based on Judd–Ofelt theory, the intensity parameter $\Omega_2$ was evaluated to investigate the change of the environment around $Eu^{3+}$ in samples with and without QDs.

*Keywords:* D. Glass ceramics; C. Optical properties; $Eu^{3+}$ ions

## 1. Introduction

In recent years, rare earth (RE) ions doped semiconductor quantum dots (QDs) have attracted an increasing attention because of their novel optical properties potentially applicable in flat plane displays, biosensors, and so on [1–3]. Generally, RE luminescence in this new class of nano-materials might be efficiently sensitized by QDs host, which is an effective way to overcome the low absorptions of parity-forbidden f–f transitions of RE ions [4–6]. However, QDs might continuously grow and agglomerate during storage, which restricts their practical applications [7,8]. A good solution would be the RE ions doped glass ceramics with semiconductor QDs embedding among an oxide glassy matrix. Such materials possess not only the merits of glassy matrix, such as excellent chemical and mechanical performance and flexibility in size and shape, but also unique physical properties originating from the semiconductors QDs, for instance, quantum confinement and size-dependent optical properties.

ZnO is a well-know wide band gap semiconductor ($E_g = 3.37$ eV [9]) and a desirable candidate as the host material for luminescence centers [10,11]. The optical properties of the ZnO nano-crystals doped with various RE species have been previously studied, which indicated that energy transfer from the host to RE ions may take place when the synthesis and microstructure of the material are well designed and controlled [10–13]. In this paper, the $Eu^{3+}$ doped glass ceramics embedding various contents of ZnO QDs were successfully prepared by a sol–gel method, and their structures and optical properties were investigated.

## 2. Experiments

The sol was prepared in two parts. For the first one, ethyl orthosilicate (TEOS), distilled water and ethanol were mixed in a molar ratio of 1:10:4. Europium nitrate was used as the $Eu^{3+}$ source, and traces of nitric acid were added as a catalyst for the hydrolysis. The mixture solution was stirred for 4 h at room temperature to complete the hydrolysis. For the second one, zinc acetate di-hydrate and ethanolamine were dissolved in isopropanol with a molar ratio of 1:1:2.5. The sols were formed after continuous stirring the solutions at 65 °C for 4 h. Two parts of sols were slowly mixed together and stirred for another 4 h, resulting in a clear sol which was then poured into vessels to form gels. The gels were then aged at room temperature for one week, and finally dried at different

---

* Corresponding author. Tel.: +86 591 8370 5402; fax: +86 591 8370 5402.
*E-mail address:* yswang@fjirsm.ac.cn (Y. Wang).

0272-8842/$36.00 © 2010 Elsevier Ltd and Techna Group S.r.l. All rights reserved.
doi:10.1016/j.ceramint.2009.12.007

temperatures (30–200 °C) for another one week to obtain bulk xerogels with compositions of $x$ZnO-(100 − $x$)SiO$_2$:$y$Eu$^{3+}$ (in mol%, $x = 0$, 5, 10, 15, 20; $y = 1$, 2, respectively). To precipitate the ZnO QDs, the xerogels were heat-treated at 500 °C for 2 h. The final samples were transparent bulk monolithic pieces.

The microstructures of the samples were investigated by transmission electron microscopy (TEM, JEM-2010) operated at 200 kV. TEM specimens were prepared by dispersing fine power grinded from bulk sample in ethanol, followed by ultrasonic agitation, and then depositing onto a carbon enhanced copper grid. The transmittance spectra were recorded in an UV near-infrared spectrophotometer (Lambda900). The photoluminescence excitation (PLE) and photoluminescence (PL) spectra, under the excitation of a xenon lamp equipped with a grating monochromator, were recorded by a PMT detector (R928).

## 3. Results and discussions

TEM micrograph of the as-made xerogel with composition of 1Eu$^{3+}$:90SiO$_2$–10ZnO is exhibited in Fig. 1a, demonstrating a typical amorphous structure. After heat-treated at 500 °C for 2 h, the homogenously distributed ZnO spherical crystallites with 3–6 nm in size precipitated from the glassy matrix, as shown in Fig. 1b. Fig. 2 reveals that, despite the difference in refractive index between the ZnO QDs (~2.0) and the surrounding glassy matrix (~1.55), the transmittance of the glass ceramic reaches as high as 90% in the visible-infrared range, which is due to the much smaller size of the precipitated crystals than the wavelength of the visible light [14,15].

The excitation spectra monitored at 614 nm (Eu$^{3+}$:$^5D_0 \rightarrow {}^7F_2$ transition) for the 1 mol% Eu$^{3+}$ doped glass ceramics embedding various contents of ZnO QDs are displayed in Fig. 3. Several peaks ascribing to Eu$^{3+}$ transitions are observed in all the samples, while a broad UV band appears in the samples with ZnO QDs, owing to the generation of excitons in the ZnO QDs and subsequent energy transfer to Eu$^{3+}$ ions residing in the QDs or near them [16]. It is noted that the center of the broad UV bands does not shift obviously with increasing ZnO content, suggesting that the band gap of QDs, related to the size of the QDs, keeps almost unchanged. This is in agreement with TEM observations where the mean grain radius remains almost a constant for the samples with different ZnO contents.

The PL spectra for the 1 and 2 mol% Eu$^{3+}$ doped samples containing various contents of ZnO were measured under excitation at 330 nm. The intensities of Eu$^{3+}$ emission at 614 nm as functions of ZnO content for the samples doped with 1 and 2 mol% Eu$^{3+}$, respectively, are displayed in Fig. 4. For the 1 mol% Eu$^{3+}$ doped samples, the emission intensifies with increasing of ZnO content from 0 to 15%, and it remains nearly constant when ZnO content further extends to 20 mol%. Interestingly, for the 2 mol% Eu$^{3+}$ doped samples, the emission intensity enhances monotonously with increasing of ZnO content from 0 to 20 mol%. These results suggest that the

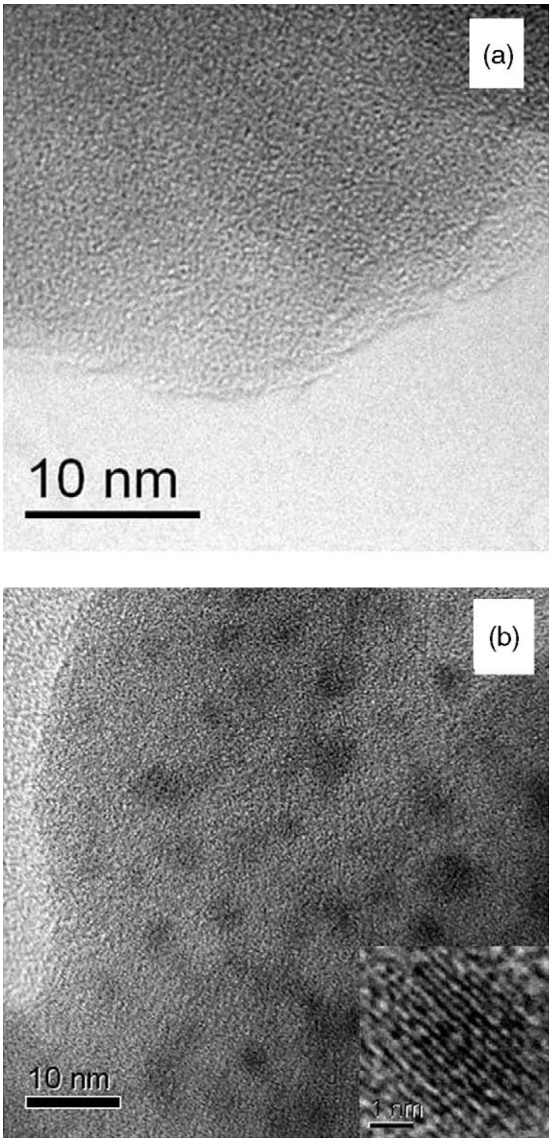

Fig. 1. TEM micrographs of (a) the as-made dry xerogel, and (b) the glass ceramic. Inset in (b) shows the HRTEM image of an individual ZnO QD.

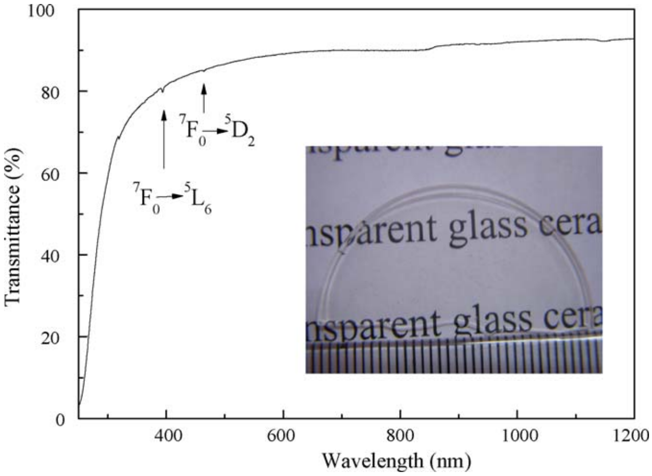

Fig. 2. Transmittance spectrum of the glass ceramic; inset shows photograph of the corresponding sample.

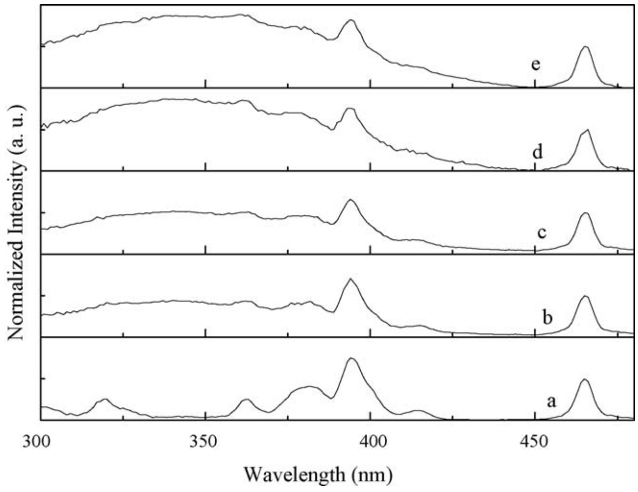

Fig. 3. Excitation spectra of 1 mol% $Eu^{3+}$ doped glass ceramics containing (a) 0; (b) 5; (c) 10; (d) 15; and (e) 20 mol% ZnO.

energy transfer between the QDs and the $Eu^{3+}$ ions is affected by both contents of ZnO and $Eu^{3+}$. For the samples with definite $Eu^{3+}$ content, with increasing of ZnO content, the amount of energy transferred from ZnO to $Eu^{3+}$ increases, resulting naturally in the intensification of the $Eu^{3+}$ emission. However, when the content ratio of ZnO/$Eu^{3+}$ excesses a certain value, the energy transfer from ZnO QDs to $Eu^{3+}$ ions is saturated. Noticeably, when the ZnO content exceeds 10 mol%, the enhanced emission intensity for the 2 mol% $Eu^{3+}$ doped sample is obviously lower than that for the 1 mol% $Eu^{3+}$ doped one, which is ascribed to the concentration quenching induced by the ion–ion interactions of $Eu^{3+}$.

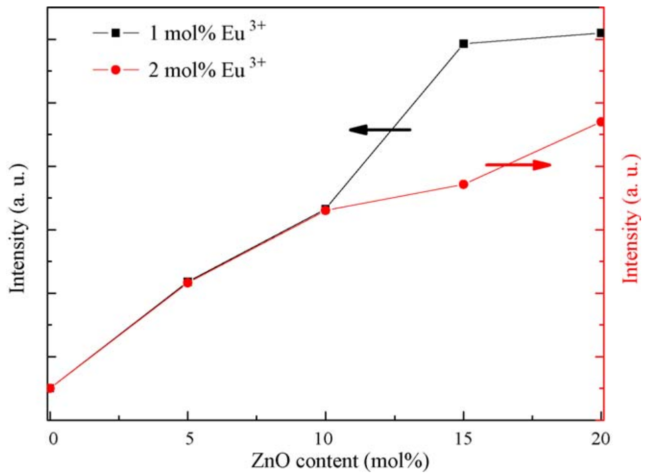

Fig. 4. $Eu^{3+}$ emission intensities at 614 nm for samples doped with 1 and 2 mol% $Eu^{3+}$ as function of ZnO content, respectively.

The Judd–Ofelt parameters are usually used to reveal the structural changes surrounding the RE ions. Due to the very low oscillator strength of the $Eu^{3+}$ 4f–4f transitions, the Judd–Ofelt intensity parameters $\Omega_t$ ($t = 2, 4, 6$) can not be obtained from the absorption spectrum. Instead, they can be determined from the emission spectra [17]. The spontaneous emission probabilities, $A_{0J}$, of the $^5D_0 \rightarrow {}^7F_J$ ($J = 2, 4, 6$) transition can be calculated by the following equation: [18]

$$A_{0J} = \frac{64e^2\pi^4}{3h\lambda_{0J}{}^3}\frac{1}{(2J+1)}\left[\frac{n(n^2+2)^2}{9}\right]\sum_{t=2,4,6}\Omega_t|\langle||U^t||\rangle|^2$$

where $e$ is the electronic charge, $h$ the Planck's constant, $\lambda$ the average wavelength of the transition, $n$ the refractive index, $\Omega_t$ the intensity parameters and $|\langle||U^t||\rangle|^2$ the squared reduced matrix elements whose values are independent of the chemical environment of the ions [19]. In the case of $Eu^{3+}$, $\Omega_t$ calculation from emission spectrum is possible since $A_{02}$, $A_{04}$, and $A_{06}$ only depend on $\Omega_2$, $\Omega_4$, and $\Omega_6$, respectively. The magnetic dipole $^5D_0 \rightarrow {}^7F_1$ transition is relatively insensitive to the chemical environment around the $Eu^{3+}$ ions, so it can be considered as a reference for the whole spectrum. The coefficient of the $Eu^{3+}$ spontaneous emission is calculated by the relation [20] of

$$A_{0J} = A_{01}\frac{I_{0J}}{I_{01}}\frac{\nu_{01}}{\nu_{0J}}$$

where $A_{01}$ is the magnetic dipole transition rate assumed constant and it is calculated using $A_{01} = n^3(A_{01})_{\rm vac}$ and $(A_{01})_{\rm vac} = 14.65\ s^{-1}$, $I_{0J}$ and $\nu_{0J}$ the emission intensity and the average frequency of the $0 \rightarrow J$ transition, respectively. The values of the Judd–Ofelt parameter ($\Omega_2$) are evaluated to be $31.8 \times 10^{-20}$ and $30.7 \times 10^{-20}\ cm^2$ for the samples with (20 mol%) and without ZnO QDs. The nearly identical values for $\Omega_2$ parameters indicates that the $Eu^{3+}$ ions environment in the two samples is similar, i.e., $Eu^{3+}$ ions are mainly located in the glass matrix and/or the interfaces between $SiO_2$ and ZnO QDs.

The time-resolved emission spectra for the 1 mol% $Eu^{3+}$ doped glass ceramic containing 20 mol% ZnO QDs is presented in Fig. 5. Different from the PL spectra without decay time, the broad emission band corresponding to the ZnO QDs disappears, remaining only some sharp peaks attributed to the $Eu^{3+}$ $^5D_0 \rightarrow {}^7F_J$ ($J = 0, 1, 2, 3, 4$) transitions for the time-resolved PL

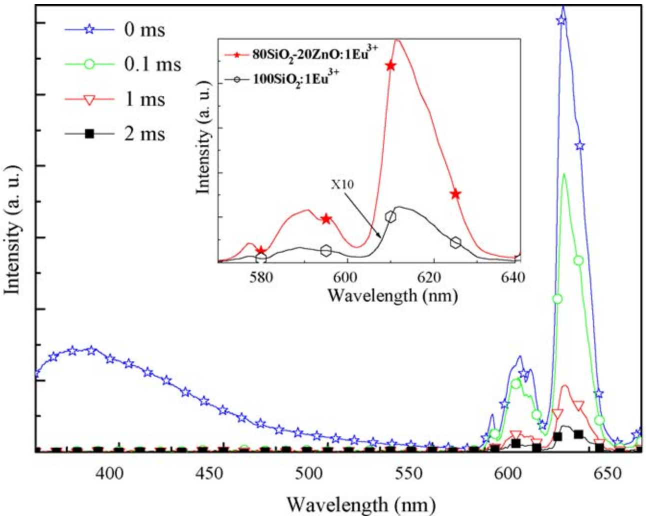

Fig. 5. Time-resolved emission spectra of 1 mol% $Eu^{3+}$ doped glass ceramic embedding 20 mol% ZnO under 330 nm excitation. Inset shows 0.1 ms-decayed spectra of 1 mol% $Eu^{3+}$ doped glass with and without ZnO.

spectra with decay time from 0.1 to 2 ms. This is due to the luminescence lifetime of ZnO (about several ns) much shorter than that of $Eu^{3+}$ (about several ms). However, the line shape of the emission peaks keeps unchanged with the decay time, suggesting that the emissions are originated from the same $Eu^{3+}$ ions. Significantly, the $Eu^{3+}$ 614 nm emission intensity in the sample with 20 mol% ZnO QDs is about 36 times stronger than that in the sample without ZnO QDs, as shown in the inset of Fig. 5.

## 4. Conclusions

The $Eu^{3+}$ doped $SiO_2$–ZnO glass ceramics were fabricated with a large range of ZnO content. The size of the ZnO quantum dots was 3–6 nm, independent on the ZnO content. The $Eu^{3+}$ visible emissions intensified remarkably with increasing of ZnO content in the sample. The near identical value of the Judd–Ofelt's intensity parameter $\Omega_2$ for the samples with and without ZnO quantum dots suggests that the $Eu^{3+}$ ions located mainly in the glass matrix and/or the interfaces between $SiO_2$ and ZnO.

## Acknowledgments

This work was supported by the National Natural Science Foundation of China (50672098), the Major Science & Technology Project of Fujian (2007HZ0002-2), the State Key Laboratory of Structural Chemistry (20080039), and the Youth Scientific Foundation of Fujian (2008F3114).

## References

[1] J. Bang, H. Yang, P.H. Holloway, Enhanced luminescence of $SiO_2$:$Eu^{3+}$ by energy transfer from ZnO nanoparticles, The Journal of Chemical Physics 123 (8) (2005) 084709.

[2] T. Moon, S.T. Hwang, D.R. Jung, D. Son, C. Kim, J. Kim, M. Kang, B. Park, Hydroxyl-quenching effects on the photoluminescence properties of $SnO_2$:$Eu^{3+}$ nanoparticles, The Journal of Physics Chemical C 111 (38) (2007) 4164–4167.

[3] Y. Liu, W. Luo, R. Li, X. Chen, Spectroscopic evidence of the multiple-site structure of $Eu^{3+}$ ions incorporated in ZnO nanocrystals, Optics Letters 32 (5) (2007) 566–568.

[4] J. Vela, B.S. Prall, P. Rastogi, D.J. Werder, J.L. Casson, D.J. Williams, V.I. Klimov, J.A. Hollingsworth, Sensitization and protection of lanthanide ion emission in $In_2O_3$:$Eu^{3+}$ nanocrystal quantum dots, The Journal of Physics Chemical C 112 (51) (2008) 20246–20250.

[5] L. Li, H.K. Yang, B.K. Moon, Z. Fu, C. Guo, J.H. Jeong, S.S. Yi, K. Jang, H.S. Lee, Photoluminescence properties of $CeO_2$:$Eu^{3+}$ nanoparticles synthesized by a sol–gel method, The Journal of Physics Chemical C 113 (2) (2009) 610–617.

[6] R.S. Ningthoujam, V. Sudarsan, $SnO_2$:$Eu^{3+}$ nanoparticles dispersed in $TiO_2$ matrix: improved energy transfer between semiconductor host and $Eu^{3+}$ ions for the low temperature synthesized samples, Applied Physics Letters 90 (17) (2007) 173113.

[7] S. Monticone, R. Tufeu, A.V. Kanaev, Complex nature of the UV and visible fluorescence of colloidal ZnO nanoparticles, The Journal of Physics Chemical B 102 (16) (1998) 2854–2862.

[8] L. Spanhel, M.A. Anderson, Semiconductor clusters in the sol–gel process: quantized aggregation, gelation, and crystal growth in concentrated zinc oxide colloids, Journal of the American Chemical Society 113 (8) (1991) 2826.

[9] Y.F Chen, N.T. Tuan, Y. Segawa, H.J. Ko, S.T. Hong, T. Yao, Stimulated emission and optical gain in ZnO epilayers grown by plasma-assisted molecular-beam epitaxy with buffers, Applied Physics Letters 78 (11) (2001) 1469–1471.

[10] A. Ishizumi, Y. Kanemitsu, Structural and luminescence properties of Eu-doped ZnO nanorods fabricated by a microemulsion method, Applied Physics Letters 86 (25) (2005) 253106.

[11] P.A. Tanner, L.X. Yu, Photoluminescence of ZnO:$Eu^{3+}$ nanoflowers, Journal of Nanoscience and Nanotechnology 8 (3) (2008) 1307–1311.

[12] A.S. Pereira, M.J. Soares, E. Alves, A. Neves, T. Monteiro, T. Trindade, Synthesis, surface modification and optical properties of $Tb^{3+}$ doped ZnO nanocrystals, Nanotechnology 17 (3) (2006) 834–839.

[13] W Jia, K. Monge, F. Fernandez, Energy transfer from the host to $Eu^{3+}$ in ZnO, Optical Materials 23 (1–2) (2003) 27–32.

[14] S. Hendy, Light scattering in transparent glass ceramics, Applied Physics Letters 81 (7) (2002) 1171–1173.

[15] M. Mattarelli, M. Montagna, P. Verrocchio, Ultratransparent glass ceramics: the structure factor and the quenching of the Rayleigh scattering, Applied Physics Letters 91 (6) (2007) 061911.

[16] A. Chiappini, C. Armellini, A. Chiasera, M. Ferrari, R. Guider, Y. Jestin, L. Minati, E. Moser, G. Nunzi Conti, S. Pelli, R. Retoux, G.C. Righini, G. Speranza, Preparation and characterization of ZnO particles embedded in organic–inorganic planar waveguide by sol–gel route, Journal of Non-Crystalline Solids 355 (18–21) (2009) 1132–1135.

[17] C. Peng, H. Zhang, J. Yu, Q. Meng, L. Fu, H. Li, L. Sun, X. Guo, Synthesis, characterization, and luminescence properties of the ternary europium complex covalently bonded to mesoporous SBA-15, The Journal of Chemical Physics B 109 (32) (2005) 15278.

[18] T.Y. Ivanova, A.A. Man'shina, A.V. Kurochkin, Y.S. Tver'yanovich, V.B. Smirnov, $Er^{3+}$ to glass matrix energy transfer in Ga-Ge-S:$Er^{3+}$ system, Journal of Non-Crystalline Solids 298 (1) (2002) 7–14.

[19] W.T. Carnal, P.R. Fields, K. Rajnak, Electronic energy levels in the trivalent lanthanide aquo ions. I. $Pr^{3+}$, $Nd^{3+}$, $Pm^{3+}$, $Sm^{3+}$, $Dy^{3+}$, $Ho^{3+}$, $Er^{3+}$, and $Tm^{3+}$, The Journal of Chemical Physics 49 (10) (1968) 4424–4442.

[20] L. Liu, X. Chen, Energy levels, fluorescence lifetime and Judd–Ofelt parameters of $Eu^{3+}$ in $Gd_2O_3$ nanocrystals, Nanotechnology 18 (25) (2007) 255704.